



## Supplementary Material for **Quantum spin Hall effect of light**

Konstantin Y. Bliokh,\* Daria Smirnova, Franco Nori\*

\*Corresponding author. E-mail: k.bliokh@gmail.com (K.Y.B.); fnori@riken.jp (F.N.)

Published 26 June 2015, *Science* **348**, 1448 (2015)  
DOI: 10.1126/science.aaa9519

**This PDF file includes:**

Supplementary Text  
Figs. S1 to S3  
Full Reference List

## Supplementary Text

### Evanescent modes and transverse spin in the Dirac equation

One of the basic models of 3D topological insulators is based on the Dirac equation for a relativistic electron (31, 32). Therefore, we provide here an analysis of evanescent Dirac waves and their spin properties.

We write the 3D Dirac equation in the standard representation in units with  $\hbar = c = 1$ :

$$i\partial_t\psi = (\boldsymbol{\alpha} \cdot \hat{\mathbf{p}} + \beta m)\psi, \quad (\text{S1})$$

where  $\psi(\mathbf{r}, t)$  is the Dirac bispinor,  $\hat{\mathbf{p}} = -i\nabla_{\mathbf{r}}$  is the momentum operator, and  $m$  is the mass. We also used the  $4 \times 4$  Dirac matrices:

$$\boldsymbol{\alpha} = \begin{pmatrix} \mathbf{0} & \boldsymbol{\sigma} \\ \boldsymbol{\sigma} & \mathbf{0} \end{pmatrix}, \quad \beta = \begin{pmatrix} \mathbf{I} & \mathbf{0} \\ \mathbf{0} & -\mathbf{I} \end{pmatrix},$$

where  $\boldsymbol{\sigma}$  are the Pauli matrices

$$\sigma_x = \begin{pmatrix} 0 & 1 \\ 1 & 0 \end{pmatrix}, \quad \sigma_y = \begin{pmatrix} 0 & -i \\ i & 0 \end{pmatrix}, \quad \sigma_z = \begin{pmatrix} 1 & 0 \\ 0 & -1 \end{pmatrix},$$

and  $\mathbf{I}$  and  $\mathbf{0}$  are the  $2 \times 2$  identity and null matrices.

The plane-wave solutions of Eq. (S1) can be written as (34)

$$\psi_{\mathbf{p}}(\mathbf{r}, t) = W(\mathbf{p}) \exp[i(\mathbf{p} \cdot \mathbf{r} - Et)], \quad (\text{S2})$$

$$W(\mathbf{p}) = \frac{1}{\sqrt{2}} \begin{pmatrix} \sqrt{1 + \frac{m}{E}} w \\ \sqrt{1 - \frac{m}{E}} \frac{\boldsymbol{\sigma} \cdot \mathbf{p}}{p} w \end{pmatrix}. \quad (\text{S3})$$

Here  $E = \pm\sqrt{p^2 + m^2}$  corresponds to two spin-degenerate energy bands (i.e., four bands

in total), and  $w = \begin{pmatrix} w_1 \\ w_2 \end{pmatrix}$ ,  $w^\dagger w = 1$ , is the normalized 2-component polarization spinor,

which determines the spin state of the electron in its rest frame.

The spin density in Dirac waves can be obtained using the canonical spin operator

$\boldsymbol{\Sigma} = \frac{1}{2} \begin{pmatrix} \boldsymbol{\sigma} & \mathbf{0} \\ \mathbf{0} & \boldsymbol{\sigma} \end{pmatrix}$ . In particular, the spin density in the plane wave (S2) and (S3) is

$$\mathbf{S} = \psi^\dagger \boldsymbol{\Sigma} \psi = \frac{m}{E} \mathbf{s} + \left(1 - \frac{m}{E}\right) \frac{\mathbf{p}(\mathbf{p} \cdot \mathbf{s})}{p^2}, \quad (\text{S4})$$

where  $\mathbf{s} = \frac{1}{2} w^\dagger \boldsymbol{\sigma} w$  characterizes the electron spin in the rest frame (34).

The evanescent-wave solution of Eq. (S1) can be written as a plane wave (S2) and (S3) with a complex momentum  $\mathbf{p}$ . Assuming an evanescent wave propagating in the  $z$ -direction and decaying in the positive  $x$ -direction, we have  $\mathbf{p} = p_z \bar{\mathbf{z}} + i\kappa \bar{\mathbf{x}}$ , where  $p_z^2 - \kappa^2 = p^2 = E^2 - m^2$ . Substituting this in Eqs. (S2) and (S3), we obtain

$$\psi_{\text{evan}} = W_{\text{evan}} \exp\left[i(p_z z - Et) - \kappa x\right], \quad (\text{S5})$$

$$W_{\text{evan}} = \frac{1}{\sqrt{2}} \begin{pmatrix} \sqrt{1+m/E} w_1 \\ \sqrt{1+m/E} w_2 \\ \sqrt{1-m/E} (p_z w_1 + i\kappa w_2) / p \\ \sqrt{1-m/E} (i\kappa w_1 - p_z w_2) / p \end{pmatrix}. \quad (\text{S6})$$

We now calculate the spin density in the Dirac evanescent wave (S5) and (S6) akin to Eq. (S4). Representing the result in the general vector form yields

$$\mathbf{S} = \psi_{\text{evan}}^\dagger \boldsymbol{\Sigma} \psi_{\text{evan}} = \mathbf{S}_w + \mathbf{S}_\perp, \quad (\text{S7})$$

$$\mathbf{S}_w = \left\{ \frac{m}{E} \mathbf{s} + \left(1 - \frac{m}{E}\right) \frac{\text{Re} \mathbf{p} (\text{Re} \mathbf{p} \cdot \mathbf{s})}{(\text{Re} \mathbf{p})^2} - \left(1 - \frac{m}{E}\right) \frac{(\text{Re} \mathbf{p} \times \text{Im} \mathbf{p}) [(\text{Re} \mathbf{p} \times \text{Im} \mathbf{p}) \cdot \mathbf{s}]}{p^2 (\text{Re} \mathbf{p})^2} \right\} e^{-2\text{Im} \mathbf{p} \cdot \mathbf{r}}, \quad (\text{S8})$$

$$\mathbf{S}_\perp = \frac{1}{2} \left(1 - \frac{m}{E}\right) \frac{\text{Re} \mathbf{p} \times \text{Im} \mathbf{p}}{p^2} e^{-2\text{Im} \mathbf{p} \cdot \mathbf{r}}. \quad (\text{S9})$$

This is a very interesting result, where we separated two distinct contributions  $\mathbf{S}_w$  and  $\mathbf{S}_\perp$ . The first one, Eq. (S8), depends on the polarization spinor  $w$  via the rest-frame spin vector  $\mathbf{s}$ , akin to the usual propagating-wave spin (S4). The second contribution, Eq. (S9), is a transverse spin, which is independent of the polarization and is entirely similar to the transverse spin in evanescent electromagnetic waves (20, 21), Eq. (5). Note that, unlike the electromagnetic-wave case, the polarization-dependent spin  $\mathbf{S}_w$  can also have a transverse component in the direction of  $(\text{Re} \mathbf{p} \times \text{Im} \mathbf{p})$ .

Thus, the above results show that the polarization-independent transverse spin  $\mathbf{S}_\perp$  equally appears in evanescent waves in Maxwell and Dirac equations, Eqs. (5) and (S9).

## Jackiw-Rebbi surface modes of the Dirac equation

A planar interface between two half-spaces, where ‘electrons’ are described by the Dirac equations with positive and negative masses, supports topological surface states. These modes are known as Jackiw-Rebbi solutions (31, 32, 35), see Fig. S1.

We consider the  $x=0$  interface separating two regions with different electron masses:

$$m(x) = \begin{cases} m_1 > 0 & \text{for } x > 0 \\ m_2 < 0 & \text{for } x < 0 \end{cases}. \quad (\text{S10})$$

The surface-state solutions have the form

$$\psi_{\text{surf}} = W_{\text{surf}} \exp\left[i(p_z z - Et) - \kappa_{1,2}|x|\right], \quad (\text{S11})$$

where  $p_z^2 - \kappa_{1,2}^2 = E^2 - m_{1,2}^2$  and the “1,2” subscripts correspond to the  $x > 0$  and  $x < 0$  half-spaces, respectively. Substituting Eq. (S11) into the Dirac equations (S1) with (S10), we find the decay factors  $\kappa_1 = m_1$  and  $\kappa_2 = -m_2$ , as well as the dispersion relation  $p_z = \pm E$ , similar to the light cone. Hereafter, the “ $\pm$ ” (or “ $\mp$ ”) signs indicate waves propagating in the positive and negative  $z$ -directions. The polarization bi-spinor of the mode (S11) can be written as

$$W_{\text{surf}} = \frac{1}{2\sqrt{N}} \begin{pmatrix} 1 \\ \mp i \\ \pm 1 \\ i \end{pmatrix}. \quad (\text{S12})$$

Here  $N = \frac{m_1 + |m_2|}{2m_1|m_2|}$  is chosen for the normalization  $\int_{-\infty}^{\infty} \psi_{\text{surf}}^\dagger \psi_{\text{surf}} dx = 1$ .

The bi-spinor (S12) corresponds to the polarization spinor  $w_{\text{surf}} = \frac{1}{\sqrt{2}} \begin{pmatrix} 1 \\ \mp i \end{pmatrix}$ , i.e.,

the rest-frame spin  $\mathbf{s}_{\text{surf}} = \mp \frac{1}{2} \bar{\mathbf{y}}$ . Thus, the rest-frame spin of the surface Jackiw-Rebbi mode is purely transverse, and opposite spins  $s_y < 0$  and  $s_y > 0$  are attached to the opposite directions of propagation  $p_z > 0$  and  $p_z < 0$ . Moreover, the forward- and backward-propagating waves have orthogonal polarization spinors  $w_{\text{surf}}$ . This is intimately related to the fact that the topological Jackiw-Rebbi modes represent helical massless fermions, which have suppressed backscattering and are robust against disorder (7, 8).

The above features are usually interpreted as spin-momentum locking in the quantum spin Hall effect and 3D topological insulators. However, quite surprisingly, the total spin density (S7)–(S9) vanishes identically in the Jackiw-Rebbi mode:

$$\mathbf{S}_{\text{surf}} = \psi_{\text{surf}}^\dagger \boldsymbol{\Sigma} \psi_{\text{surf}} \equiv 0. \quad (\text{S13})$$

This happens because the transverse polarization-independent spin (S9) exactly cancels the polarization-dependent contribution (S8) for the above polarization:

$$\mathbf{S}_\perp = -\mathbf{S}_w = \pm \frac{1}{2N} \frac{Em_{1,2}}{(E + m_{1,2})^2} \bar{\mathbf{y}} e^{-2m_{1,2}x}. \quad (\text{S14})$$

Since both contributions above are locked to the momentum (as in the quantum spin Hall effect), one can say that opposite spin-momentum locking appears in the two spin contributions, while the total spin vanishes. Thus, the surface modes of the Dirac equation exhibit remarkable topological properties but do not provide any spin transport, i.e., the quantum spin Hall effect.

The cancellation of the spin in the Jackiw-Rebbi modes can be explained by the fact that the  $m_1 = -m_2$  interface does not break spatial-inversion ( $\mathcal{P}$ ) symmetry. Indeed, the  $\mathcal{P}$  transformation results in the global change of the sign of the mass, which is not detectable. At the same time, the quantum spin Hall effect has broken inversion symmetry: it flips momenta but not spins. Thus, the quantum spin Hall effect is possible only in systems with broken inversion symmetry, such as the optical interfaces considered below.

For completeness, we determine the integral values of the two transverse spin contributions (S14). Denoting  $\langle \dots \rangle \equiv \int_{-\infty}^{\infty} \dots dx$ , we obtain

$$\langle \mathbf{S}_\perp \rangle = -\langle \mathbf{S}_w \rangle = \pm \frac{1}{2} \frac{Em_1 m_2 (2E + m_1 + m_2)}{(E + m_1)^2 (E + m_2)^2} \bar{\mathbf{y}}. \quad (\text{S15})$$

## Surface waves in Maxwell equations

Free-space Maxwell equations describe photons, i.e., massless spin-1 particles. These equations can also be written in the Dirac-like form with electric and magnetic fields forming an effective wavefunction (36). For simplicity, in what follows we use natural electro-dynamical units with  $\epsilon_0 = \mu_0 = c = 1$ . The light-cone spectrum  $\omega = k$  and bulk plane-wave solutions for Maxwell equations in vacuum are well-known. The complex electric-field amplitude of a plane wave is given by Eq. (1), whereas the corresponding magnetic field is  $\mathbf{H} = \frac{\mathbf{k}}{k} \times \mathbf{E}$ . The spin angular momentum of light is described by the following spin-1 operator (16, 21, 36):

$$\hat{S}_x = -i \begin{pmatrix} 0 & 0 & 0 \\ 0 & 0 & 1 \\ 0 & -1 & 0 \end{pmatrix}, \quad \hat{S}_y = -i \begin{pmatrix} 0 & 0 & -1 \\ 0 & 0 & 0 \\ 1 & 0 & 0 \end{pmatrix}, \quad \hat{S}_z = -i \begin{pmatrix} 0 & 1 & 0 \\ -1 & 0 & 0 \\ 0 & 0 & 0 \end{pmatrix}. \quad (\text{S16})$$

Using the operator  $\hat{\Sigma} = \begin{pmatrix} \hat{S} & \mathbf{0} \\ \mathbf{0} & \hat{S} \end{pmatrix}$  and the “wavefunction”  $\psi = \frac{1}{2\sqrt{\omega}} \begin{pmatrix} \mathbf{E} \\ \mathbf{H} \end{pmatrix}$ , normalized as  $\psi^\dagger \psi = 1$ , we obtain the spin density in a plane electromagnetic wave (1):

$$\mathbf{S} = \psi^\dagger \hat{\Sigma} \psi = \sigma \frac{\mathbf{k}}{k}. \quad (\text{S17})$$

In addition to the propagating “bulk” modes, Maxwell equations can also exhibit surface modes at interfaces between two homogeneous media with different electric permittivities  $\epsilon_{1,2}$  and permeabilities  $\mu_{1,2}$ . In the generic case, such an interface breaks the so-called dual symmetry between the electric and magnetic properties (29, 37, 38). Therefore, instead of the circularly-polarized helicity eigenstates in free space, the eigenpolarizations of the surface modes are the transverse-electric (TE) and transverse-magnetic (TM) linearly-polarized waves. Considering waves propagating in the  $(x,z)$ -plane of a homogeneous medium, the full Maxwell equations can be reduced to uncoupled 2D scalar wave equations for the normal components  $E_y$  (TE mode) and  $H_y$  (TM mode):

$$\begin{aligned} \Delta E_y + \epsilon \mu \omega^2 E_y &= 0 & (\text{TE}), \\ \Delta H_y + \epsilon \mu \omega^2 H_y &= 0 & (\text{TM}), \end{aligned} \quad (\text{S18})$$

where  $\Delta = \frac{\partial^2}{\partial x^2} + \frac{\partial^2}{\partial z^2}$  and the other nonzero field components are determined by

$$H_z = -\frac{i}{\mu \omega} \frac{\partial E_y}{\partial x}, \quad H_x = \frac{i}{\mu \omega} \frac{\partial E_y}{\partial z} \quad (\text{TE}),$$

$$E_z = \frac{i}{\varepsilon\omega} \frac{\partial H_y}{\partial x}, \quad E_x = -\frac{i}{\varepsilon\omega} \frac{\partial H_y}{\partial z} \quad (\text{TM}). \quad (\text{S19})$$

Consider now the  $x = 0$  interface between two homogeneous media:

$$\varepsilon(x), \mu(x) = \begin{cases} \varepsilon_1, \mu_1 & \text{for } x > 0 \\ \varepsilon_2, \mu_2 & \text{for } x < 0 \end{cases}. \quad (\text{S20})$$

We are looking for surface modes of the interface, which have the evanescent-wave form  $\{E_y, H_y\} \propto \exp(ik_z z - \kappa_{1,2}|x|)$ , where  $\kappa_{1,2} = (k_z^2 - \varepsilon_{1,2}\mu_{1,2}\omega^2)^{1/2}$ . Supplying the wave equations with the corresponding boundary conditions (continuity of the tangential components  $E_{y,z}$  and  $H_{y,z}$ ), one can derive the following equations for the TE and TM surface modes (39, 40):

$$\begin{aligned} \frac{\kappa_1}{\mu_1} + \frac{\kappa_2}{\mu_2} &= 0 \quad (\text{TE}), \\ \frac{\kappa_1}{\varepsilon_1} + \frac{\kappa_2}{\varepsilon_2} &= 0 \quad (\text{TM}). \end{aligned} \quad (\text{S21})$$

Together with the dispersion relation  $\kappa_{1,2} = (k_z^2 - \varepsilon_{1,2}\mu_{1,2}\omega^2)^{1/2}$ , Eqs. (S21) determine the existence regions for the surface TE and TM modes (40). These regions are depicted in Fig. S2 in the  $(\varepsilon_2/\varepsilon_1, \mu_2/\mu_1)$ -plane of the relative permittivity and permeability. Importantly, the TE and TM modes cannot exist simultaneously (except for the degenerate case  $\varepsilon_2/\varepsilon_1 = \mu_2/\mu_1 = -1$ ). Therefore, instead of two polarization (spin) states of the propagating light, the surface modes of Maxwell equations have only one fixed polarization (either TE or TM) in the generic case.

The surface Maxwell modes have linear (conical) dispersion lying outside of the light cone for bulk waves. An example of such dispersion is show in Fig. S3. An interface between free space ( $\varepsilon_1 = \mu_1 = 1$ ) and a medium with  $\mu_2 = 1$  and  $\varepsilon_2 < -1$  supports TM

surface modes with the dispersion  $k_z = \pm \sqrt{\frac{\varepsilon_1 \varepsilon_2}{\varepsilon_1 + \varepsilon_2}} \omega$  (hereafter we keep  $\varepsilon_1$  for the sake of

symmetry). Note that in this case, the medium 2 does not support any bulk modes and represents a perfect ‘‘insulator’’ for photons. Therefore, no spin properties (e.g., spin Chern number, etc.) can be ascribed to the  $x < 0$  semispace. In addition, here we intentionally consider non-dispersive media with permittivities and permeabilities independent of  $\omega$ . Introducing a dispersion  $\varepsilon_2(\omega)$ , as in the case of a real metal, results in plasma-frequency longitudinal bulk modes (plasmons) and high-frequency transverse bulk modes (photons) in the medium 2. This is accompanied by the saturation of the surface-mode dispersion at lower frequencies, as shown in Fig. 3.

Both TE and TM surface modes are linearly-polarized, i.e., have zero helicity  $\sigma = 0$  and no usual spin (S16). At the same time, they possess the transverse spin (5) (20, 21).

In particular, for the above example of the vacuum-medium interface with  $\mu_2 = 1$ ,  $\epsilon_2 < -1$ , the spin of the TM surface wave is described by the canonical spin operator  $\hat{\Sigma}$  and the “wavefunction” in a medium  $\psi = \frac{1}{2\sqrt{\omega}} \begin{pmatrix} \mathbf{E}/\sqrt{\mu} \\ \mathbf{H}/\sqrt{\epsilon} \end{pmatrix}$  (21). Since the electromagnetic energy density in the medium is  $\frac{1}{4}(\epsilon|\mathbf{E}|^2 + \mu|\mathbf{H}|^2)$ , we impose the one-particle normalization  $\int_{-\infty}^{\infty} \epsilon\mu(\psi_{\text{surf}}^\dagger \psi_{\text{surf}}) dx = 1$  for the  $x$ -localized surface mode. This results in the following transverse spin density in the TM surface mode:

$$\mathbf{S}_{\text{surf}} = \psi_{\text{surf}}^\dagger \hat{\Sigma} \psi_{\text{surf}} = \pm 2\omega \frac{-\epsilon_{2,1}}{(\epsilon_2^2 - \epsilon_1^2)} \sqrt{\frac{\epsilon_1 \epsilon_2}{\epsilon_1 + \epsilon_2}} \bar{\mathbf{y}} e^{-2\kappa_{1,2}|x|}. \quad (\text{S22})$$

This spin density is purely transverse, and the opposite spin directions  $S_y > 0$  and  $S_y < 0$  are locked with the opposite propagation directions  $k_z > 0$  and  $k_z < 0$ . This is the main feature of the quantum spin Hall effect, which is emphasized in the main text of the paper. However, unlike the topological Jackiw-Rebbi modes, the surface electromagnetic modes have a fixed polarization which is independent of the momentum. In the above example, this is the TM-polarization described by the polarization spinor (Jones vector)  $\xi = \begin{pmatrix} 1 \\ 0 \end{pmatrix}$ . Thus, the surface modes of Maxwell equations are not helical fermions, they have usual scattering properties, and are not robust against disorder. Nonetheless, in contrast to the Jackiw-Rebbi modes, surface electromagnetic waves do provide robust unidirectional spin transport along the interface. Indeed, independently of the direction of propagation, the  $z$ -component of the spin current is determined by the product  $S_y k_z$ , which is always positive.

We emphasize that the transverse spin (S22) originates solely from the polarization-independent contribution  $\mathbf{S}_\perp$ , Eq. (5). Although the transverse-spin densities (S22) have opposite signs at the opposite sides of the interface, the total (i.e.,  $x$ -integrated) transverse spin is non-zero:

$$\langle \mathbf{S}_{\text{surf}} \rangle = \pm \frac{1}{\sqrt{-\epsilon_1 \epsilon_2}} \bar{\mathbf{y}}. \quad (\text{S23})$$



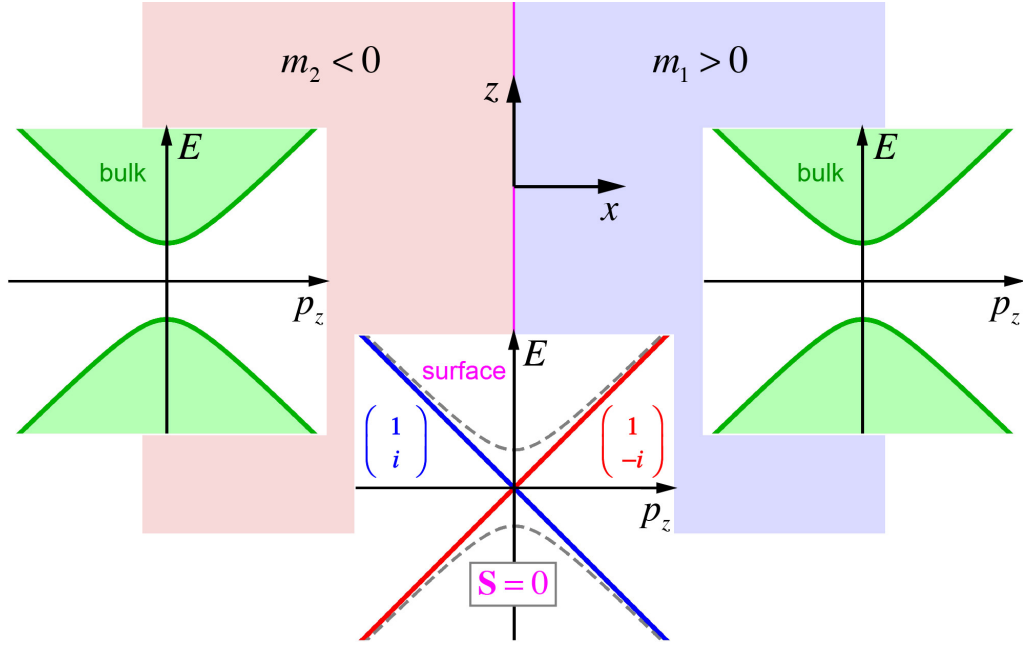


**Fig. S1.** Dispersions of the bulk and surface modes for the Dirac equation with the  $x=0$  interface separating the half-spaces with positive and negative masses. In both half-spaces the Dirac bulk modes exist, while the interface supports topological Jackiw-Rebbi modes. These surface modes exhibit transverse spinor-momentum locking related to their helical fermion nature. However, the total transverse spin vanishes identically due to the mutual cancellation of the polarization-dependent and polarization-independent contributions, Eqs. (S7)–(S9) and (S13)–(S15).

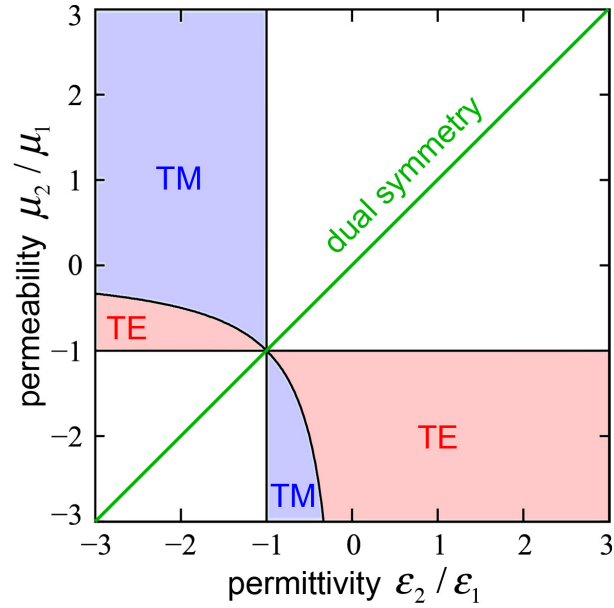


**Fig. S2.** The existence regions for surface Maxwell modes at the planar interface between two media with permittivities  $\epsilon_{1,2}$  and permeabilities  $\mu_{1,2}$ . Either transverse-electric (TE), or transverse-magnetic (TM) linearly-polarized modes, or none of these can exist at every value of the parameters. (The only exclusion is the degenerate case  $\epsilon_2/\epsilon_1 = \mu_2/\mu_1 = -1$ .) Moreover, the dual symmetry between electric and magnetic properties (shown by the green line) must be broken for the existence of surface modes of Maxwell equations.

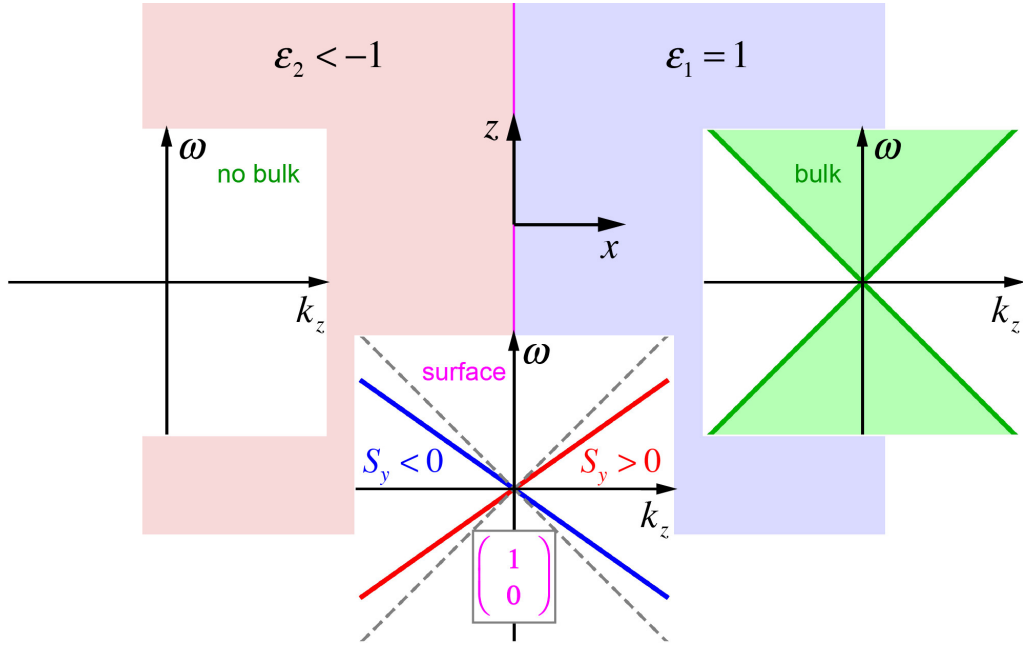


**Fig. S3.** Dispersions of the bulk and surface modes of Maxwell equations with the  $x=0$  interface separating two half-spaces with different permittivities  $\epsilon$  and the same permeability  $\mu=1$ . While the usual light represents bulk modes of the vacuum, there are no propagating waves in the medium with negative permittivity. The interface supports surface modes with the fixed TM polarization described by the Jones-vector spinor  $\xi = \begin{pmatrix} 1 \\ 0 \end{pmatrix}$ . These modes

exhibit transverse spin-momentum locking due to the transverse polarization-independent spin, Eqs. (5), (6), (S22) and (S23). This corresponds to the quantum spin Hall effect of light. Furthermore the spectrum of these modes lies outside the light cone and therefore has a non-removable degeneracy at  $k=0$ .

## References and Notes

1. M. Stone, Ed., *The Quantum Hall Effect* (World Scientific, Singapore, 1992).
2. D. J. Thouless, M. Kohmoto, M. P. Nightingale, M. den Nijs, Quantized Hall conductance in a two-dimensional periodic potential. *Phys. Rev. Lett.* **49**, 405–408 (1982).  
[doi:10.1103/PhysRevLett.49.405](https://doi.org/10.1103/PhysRevLett.49.405)
3. S. Murakami, N. Nagaosa, S.-C. Zhang, Dissipationless quantum spin current at room temperature. *Science* **301**, 1348–1351 (2003). [Medline doi:10.1126/science.1087128](https://pubmed.ncbi.nlm.nih.gov/1087128/)
4. J. Sinova, D. Culcer, Q. Niu, N. A. Sinitsyn, T. Jungwirth, A. H. MacDonald, Universal intrinsic spin Hall effect. *Phys. Rev. Lett.* **92**, 126603 (2004). [Medline doi:10.1103/PhysRevLett.92.126603](https://pubmed.ncbi.nlm.nih.gov/126603/)
5. C. L. Kane, E. J. Mele, Z<sub>2</sub> topological order and the quantum spin Hall effect. *Phys. Rev. Lett.* **95**, 146802 (2005). [Medline doi:10.1103/PhysRevLett.95.146802](https://pubmed.ncbi.nlm.nih.gov/146802/)
6. B. A. Bernevig, T. L. Hughes, S. C. Zhang, Quantum spin Hall effect and topological phase transition in HgTe quantum wells. *Science* **314**, 1757–1761 (2006). [Medline doi:10.1126/science.1133734](https://pubmed.ncbi.nlm.nih.gov/1133734/)
7. M. Z. Hasan, C. L. Kane, *Colloquium* : Topological insulators. *Rev. Mod. Phys.* **82**, 3045–3067 (2010). [doi:10.1103/RevModPhys.82.3045](https://pubmed.ncbi.nlm.nih.gov/3045/)
8. X.-L. Qi, S.-C. Zhang, Topological insulators and superconductors. *Rev. Mod. Phys.* **83**, 1057–1110 (2011). [doi:10.1103/RevModPhys.83.1057](https://pubmed.ncbi.nlm.nih.gov/1057/)
9. G. L. J. A. Rikken, B. A. van Tiggelen, Observation of magnetically induced transverse diffusion of light. *Nature* **381**, 54–55 (1996). [doi:10.1038/381054a0](https://pubmed.ncbi.nlm.nih.gov/381054a0/)
10. F. D. M. Haldane, S. Raghu, Possible realization of directional optical waveguides in photonic crystals with broken time-reversal symmetry. *Phys. Rev. Lett.* **100**, 013904 (2008). [Medline doi:10.1103/PhysRevLett.100.013904](https://pubmed.ncbi.nlm.nih.gov/013904/)
11. Z. Wang, Y. Chong, J. D. Joannopoulos, M. Soljacić, Observation of unidirectional backscattering-immune topological electromagnetic states. *Nature* **461**, 772–775 (2009). [Medline doi:10.1038/nature08293](https://pubmed.ncbi.nlm.nih.gov/08293/)
12. R. Y. Chiao, Y.-S. Wu, Manifestations of Berry's topological phase for the photon. *Phys. Rev. Lett.* **57**, 933–936 (1986). [Medline doi:10.1103/PhysRevLett.57.933](https://pubmed.ncbi.nlm.nih.gov/933/)
13. K. Y. Bliokh, Y. P. Bliokh, Topological spin transport of photons: The optical Magnus effect and Berry phase. *Phys. Lett. A* **333**, 181–186 (2004). [doi:10.1016/j.physleta.2004.10.035](https://pubmed.ncbi.nlm.nih.gov/1016/j.physleta.2004.10.035/)
14. M. Onoda, S. Murakami, N. Nagaosa, Hall effect of light. *Phys. Rev. Lett.* **93**, 083901 (2004). [Medline doi:10.1103/PhysRevLett.93.083901](https://pubmed.ncbi.nlm.nih.gov/083901/)
15. K. Y. Bliokh, A. Niv, V. Kleiner, E. Hasman, Geometrodynamics of spinning light. *Nat. Photonics* **2**, 748–753 (2008). [doi:10.1038/nphoton.2008.229](https://pubmed.ncbi.nlm.nih.gov/2008.229/)
16. K. Y. Bliokh, M. A. Alonso, E. A. Ostrovskaya, A. Aiello, Angular momenta and spin-orbit interaction of nonparaxial light in free space. *Phys. Rev. A* **82**, 063825 (2010). [doi:10.1103/PhysRevA.82.063825](https://pubmed.ncbi.nlm.nih.gov/063825/)

17. M. Hafezi, E. A. Demler, M. D. Lukin, J. M. Taylor, Robust optical delay lines with topological protection. *Nat. Phys.* **7**, 907–912 (2011). [doi:10.1038/nphys2063](https://doi.org/10.1038/nphys2063)
18. A. B. Khanikaev, S. H. Mousavi, W.-K. Tse, M. Kargarian, A. H. MacDonald, G. Shvets, Photonic topological insulators. *Nat. Mater.* **12**, 233–239 (2013). [Medline doi:10.1038/nmat3520](https://doi.org/10.1038/nmat3520)
19. M. C. Rechtsman, J. M. Zeuner, Y. Plotnik, Y. Lumer, D. Podolsky, F. Dreisow, S. Nolte, M. Segev, A. Szameit, Photonic Floquet topological insulators. *Nature* **496**, 196–200 (2013). [Medline doi:10.1038/nature12066](https://doi.org/10.1038/nature12066)
20. K. Y. Bliokh, F. Nori, Transverse spin of a surface polariton. *Phys. Rev. A* **85**, 061801 (2012). [doi:10.1103/PhysRevA.85.061801](https://doi.org/10.1103/PhysRevA.85.061801)
21. K. Y. Bliokh, A. Y. Bekshaev, F. Nori, Extraordinary momentum and spin in evanescent waves. *Nat. Commun.* **5**, 3300 (2014). [Medline doi:10.1038/ncomms4300](https://doi.org/10.1038/ncomms4300)
22. F. J. Rodríguez-Fortuño, G. Marino, P. Ginzburg, D. O’Connor, A. Martínez, G. A. Wurtz, A. V. Zayats, Near-field interference for the unidirectional excitation of electromagnetic guided modes. *Science* **340**, 328–330 (2013). [Medline doi:10.1126/science.1257671](https://doi.org/10.1126/science.1257671)
23. J. Petersen, J. Volz, A. Rauschenbeutel, Chiral nanophotonic waveguide interface based on spin-orbit interaction of light. *Science* **346**, 67–71 (2014). [Medline doi:10.1126/science.1257671](https://doi.org/10.1126/science.1257671)
24. D. O’Connor, P. Ginzburg, F. J. Rodríguez-Fortuño, G. A. Wurtz, A. V. Zayats, Spin-orbit coupling in surface plasmon scattering by nanostructures. *Nat. Commun.* **5**, 5327 (2014). [Medline doi:10.1038/ncomms6327](https://doi.org/10.1038/ncomms6327)
25. R. Mitsch, C. Sayrin, B. Albrecht, P. Schneeweiss, A. Rauschenbeutel, Quantum state-controlled directional spontaneous emission of photons into a nanophotonic waveguide. *Nat. Commun.* **5**, 5713 (2014). [Medline doi:10.1038/ncomms6713](https://doi.org/10.1038/ncomms6713)
26. B. le Feber, N. Rotenberg, L. Kuipers, Nanophotonic control of circular dipole emission. *Nat. Commun.* **6**, 6695 (2015). [Medline doi:10.1038/ncomms7695](https://doi.org/10.1038/ncomms7695)
27. I. Söllner *et al.*, arXiv:1406.4295v3 (2014).
28. D. N. Sheng, Z. Y. Weng, L. Sheng, F. D. M. Haldane, Quantum spin-Hall effect and topologically invariant Chern numbers. *Phys. Rev. Lett.* **97**, 036808 (2006). [Medline doi:10.1103/PhysRevLett.97.036808](https://doi.org/10.1103/PhysRevLett.97.036808)
29. I. Fernandez-Corbaton, X. Zambrana-Puyalto, N. Tischler, X. Vidal, M. L. Juan, G. Molina-Terriza, Electromagnetic duality symmetry and helicity conservation for the macroscopic Maxwell’s equations. *Phys. Rev. Lett.* **111**, 060401 (2013). [Medline doi:10.1103/PhysRevLett.111.060401](https://doi.org/10.1103/PhysRevLett.111.060401)
30. L. Lu, J. D. Joannopoulos, M. Soljačić, Topological photonics. *Nat. Photonics* **8**, 821–829 (2014). [doi:10.1038/nphoton.2014.248](https://doi.org/10.1038/nphoton.2014.248)
31. R. Jackiw, C. Rebbi, Solitons with fermion number 1/2. *Phys. Rev. D Part. Fields* **13**, 3398–3409 (1976). [doi:10.1103/PhysRevD.13.3398](https://doi.org/10.1103/PhysRevD.13.3398)

32. A. P. Schnyder, S. Ryu, A. Furusaki, A. W. W. Ludwig, Classification of topological insulators and superconductors in three spatial dimensions. *Phys. Rev. B* **78**, 195125 (2008). [doi:10.1103/PhysRevB.78.195125](https://doi.org/10.1103/PhysRevB.78.195125)
33. A. V. Zayats, I. I. Smolyaninov, A. A. Maradudin, Nano-optics of surface plasmon polaritons. *Phys. Rep.* **408**, 131–314 (2005). [doi:10.1016/j.physrep.2004.11.001](https://doi.org/10.1016/j.physrep.2004.11.001)
34. V. B. Berestetskii, E. M. Lifshitz, L. P. Pitaevskii, *Quantum Electrodynamics* (Pergamon, Oxford, 1982).
35. S.-Q. Shen, W.-Y. Shan, H.-Z. Lu, Topological insulator and the Dirac equation. *SPIN* **1**, 33–44 (2011). [doi:10.1142/S2010324711000057](https://doi.org/10.1142/S2010324711000057)
36. I. Bialynicki-Birula, *Prog. Opt.* **36**, 245 (1996).
37. R. P. Cameron, S. M. Barnett, A. M. Yao, Optical helicity, optical spin and related quantities in electromagnetic theory. *New J. Phys.* **14**, 053050 (2012). [doi:10.1088/1367-2630/14/5/053050](https://doi.org/10.1088/1367-2630/14/5/053050)
38. K. Y. Bliokh, A. Y. Bekshaev, F. Nori, Dual electromagnetism: Helicity, spin, momentum and angular momentum. *New J. Phys.* **15**, 033026 (2013). [doi:10.1088/1367-2630/15/3/033026](https://doi.org/10.1088/1367-2630/15/3/033026)
39. R. Ruppin, Surface polaritons of a left-handed medium. *Phys. Lett. A* **277**, 61–64 (2000). [doi:10.1016/S0375-9601\(00\)00694-0](https://doi.org/10.1016/S0375-9601(00)00694-0)
40. I. V. Shadrivov, A. A. Sukhorukov, Y. S. Kivshar, A. A. Zharov, A. D. Boardman, P. Egan, Nonlinear surface waves in left-handed materials. *Phys. Rev. E Stat. Nonlin. Soft Matter Phys.* **69**, 016617 (2004). [Medline doi:10.1103/PhysRevE.69.016617](https://doi.org/10.1103/PhysRevE.69.016617)